

Exploring the Roper wave function in Lattice QCD

Waseem Kamleh^{*†}

*Special Research Centre for the Subatomic Structure of Matter,
University of Adelaide, Australia
E-mail: waseem.kamleh@adelaide.edu.au*

Derek B. Leinweber

*Special Research Centre for the Subatomic Structure of Matter,
University of Adelaide, Australia*

Dale S. Roberts

*Special Research Centre for the Subatomic Structure of Matter,
University of Adelaide, Australia, and
National Computational Infrastructure,
Australian National University, Canberra, Australia*

Using a correlation matrix analysis consisting of a variety of smearings, the CSSM Lattice collaboration has successfully isolated states associated with the Roper resonance and other "exotic" excited states such as the $\Lambda(1405)$ on the lattice at near-physical pion masses. We explore the nature of the Roper by examining the eigenvectors that arise from the variational analysis, demonstrating that the Roper state is dominated by the χ_1 nucleon interpolator and only poorly couples to χ_2 . By examining the probability distribution of the Roper on the lattice, we find a structure consistent with a constituent quark model. In particular, the Roper d -quark wave function contains a single node consistent with a $2S$ state. A detailed comparison with constituent quark model wave functions is carried out, validating the approach of accessing these states by constructing a variational basis composed of different levels of fermion source and sink smearing.

*31st International Symposium on Lattice Field Theory - LATTICE 2013
July 29 - August 3, 2013
Mainz, Germany*

^{*}Speaker.

[†]This research was undertaken with the assistance of resources at the NCI National Facility in Canberra, Australia, provided through the National Computational Merit Allocation Scheme and the University of Adelaide Partner Share. This research is supported by the Australian Research Council.

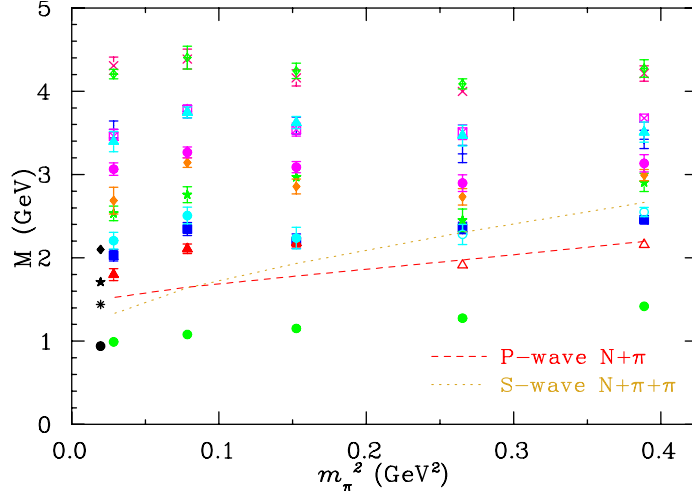


Figure 1: The even parity nucleon spectrum in full QCD from [9], resulting from the superposition of two 8×8 correlation matrix analyses. The two lowest scattering channels are shown for reference.

1. The Roper Resonance

The first positive-parity excited state of the nucleon, known as the Roper resonance, $N_{\frac{1}{2}}^{1+}$ (1440 MeV) P_{11} , has presented a long-standing puzzle since its discovery in the 1960's due to its lower mass compared to the adjacent negative parity, $N_{\frac{1}{2}}^{1-}$ (1535 MeV) S_{11} , state. In constituent quark models with harmonic oscillator potentials, the lowest-lying odd-parity state naturally occurs below the P_{11} state [1, 2]. In nature the Roper resonance is almost 100 MeV below the S_{11} state.

Using variational techniques[3, 4], the CSSM [5, 6, 7] has successfully isolated the elusive Roper [8, 9] and $\Lambda(1405)$ [10] resonances on the lattice. The highlights of the CSSM results for the even-parity nucleon spectrum in Full QCD are shown in Figure 1. These results (and the full QCD results that follow below) were calculated on the 2+1 flavour non-perturbatively improved clover configurations[11] made available by the PACS-CS collaboration via the ILDG[12]. Critical to our results is the construction of a large operator basis by considering different amounts of gauge-invariant Gaussian smearing[13].

We can see in Figure 1 that the first positive parity excited state at the two heaviest pion masses has an energy that is consistent with an $N + \pi$ multi-particle state, but as we move to light quark masses the energy of this state shows significant chiral curvature. We shall demonstrate that this state corresponds to the Roper resonance. Specifically, we identify this state with the $2S$ radial excitation of the nucleon. At the physical quark mass, the lattice Roper state sits high when compared with the experimental point at 1440 MeV. We argue that the finite volume of the lattice causes the energy of the Roper to be pushed upwards away from the physical value.

2. Variational Analysis

The success of the CSSM lattice program in identifying resonance states on the lattice is founded upon variational techniques that isolate individual excited states by constructing an operator basis that couples to the states of interest and then considering their cross-correlation matrix in

order to diagonalise the operator space. To access N states of the spectrum, we require at least N operators.

The parity-projected, two-point correlation function matrix for $\mathbf{p} = \mathbf{0}$ can be written as

$$G_{ij}^{\pm}(t) = \sum_{\mathbf{x}} \text{tr}_{\text{sp}}(\Gamma_{\pm} \langle \Omega | \chi_i(x) \bar{\chi}_j(0) | \Omega \rangle) = \sum_{\alpha=0}^{N-1} \lambda_i^{\alpha} \bar{\lambda}_j^{\alpha} e^{-m_{\alpha} t}, \quad (2.1)$$

where Γ_{\pm} are the parity-projection operators and λ_i^{α} and $\bar{\lambda}_j^{\alpha}$ are, respectively, the couplings of interpolators χ_i and $\bar{\chi}_j$ at the sink and source to eigenstates $\alpha = 0, \dots, N-1$ of mass m_{α} . The idea now is to construct N independent operators ϕ_i that isolate N baryon states $|B_{\alpha}\rangle$; that is, to find operators $\bar{\phi}^{\alpha} = \sum_{i=1}^N u_i^{\alpha} \bar{\chi}_i$ and $\phi^{\alpha} = \sum_{i=1}^N v_i^{\alpha*} \chi_i$ such that

$$\begin{aligned} \langle B_{\beta}, p, s | \bar{\phi}^{\alpha} | \Omega \rangle &= \delta_{\alpha\beta} \bar{z}^{\alpha} \bar{u}(\alpha, p, s), \text{ and} \\ \langle \Omega | \phi^{\alpha} | B_{\beta}, p, s \rangle &= \delta_{\alpha\beta} z^{\alpha} u(\alpha, p, s), \end{aligned} \quad (2.2)$$

where z^{α} and \bar{z}^{α} are the coupling strengths of ϕ^{α} and $\bar{\phi}^{\alpha}$ to the state $|B_{\alpha}\rangle$. It follows that

$$G_{ij}^{\pm}(t) u_j^{\alpha} = \lambda_i^{\alpha} \bar{z}^{\alpha} e^{-m_{\alpha} t}, \quad (2.3)$$

where, for notational convenience, we take the repeated Latin indices to be summed over while repeated Greek indices are not.

The only t dependence in Eq. (2.3) is in the exponential term, so we immediately construct the recurrence relation $G_{ij}^{\pm}(t) u_j^{\alpha} = e^{-m_{\alpha} \Delta t} G_{ik}^{\pm}(t + \Delta t) u_k^{\alpha}$, which can be written as

$$(G^{\pm}(t + \Delta t))^{-1} G^{\pm}(t) \mathbf{u}^{\alpha} = e^{-m_{\alpha} \Delta t} \mathbf{u}^{\alpha}. \quad (2.4)$$

This is an eigensystem equation for the matrix $(G^{\pm}(t + \Delta t))^{-1} G^{\pm}(t)$, with eigenvectors \mathbf{u}^{α} and eigenvalues $e^{-m_{\alpha} \Delta t}$.

Similarly, we can construct the associated left-eigensystem equation $\mathbf{v}^{\alpha\dagger} G^{\pm}(t) (G^{\pm}(t + \Delta t))^{-1} = e^{-m_{\alpha} \Delta t} \mathbf{v}^{\alpha\dagger}$, and then Eq. (2.2) implies that

$$G_{\alpha}^{\pm}(t) := \mathbf{v}^{\alpha\dagger} G^{\pm}(t) \mathbf{u}^{\alpha} = z^{\alpha} \bar{z}^{\alpha} e^{-m_{\alpha} t}. \quad (2.5)$$

Thus, the only state present in $G_{\alpha}^{\pm}(t)$ is $|B_{\alpha}\rangle$ of mass m_{α} .

3. Structure of the Roper

Having constructed an appropriate operator basis, we can examine the components of the right eigenvectors \mathbf{u}^{α} for a given state α to see how each operator contributes to the formation of that state. In Figure 2 we show the eigenvector components for the ground and first excited states in the even parity nucleon channel. We have four available smearings $n = 16, 35, 100, 200$ and two interpolating fields, χ_1 (green points) and χ_2 (blue points), giving us eight operators in total. For each operator, the eigenvector components are shown in groups of five, corresponding to each of the five pion masses $m_{\pi} = 0.156, 0.293, 0.413, 0.572, 0.702$ GeV, with pion mass increasing from left to right.

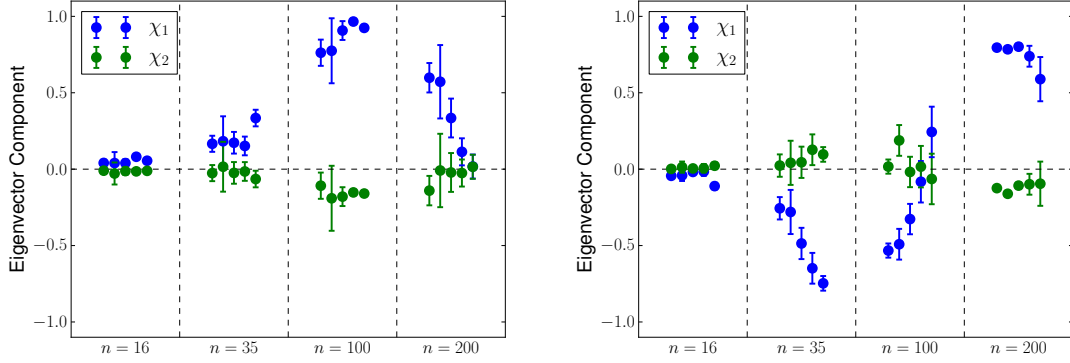


Figure 2: Eigenvector components for the nucleon ground state (left) and first excited state (right) resulting from an 8×8 correlation matrix with χ_1 , χ_2 interpolators. The blue points correspond to χ_1 components and the green to χ_2 . For each of the four smearing sweep values $n = 16, 35, 100, 200$ we display the eigenvector components at each of the five pion masses, with mass increasing from left to right.

Turning first to the left plot showing the ground state eigenmodes, we see that the only significant contributions are from χ_1 with 100 and 200 smearing sweeps. Both these operators have positive component, with the $n = 200$ contribution increasing as the quark mass decreases, which is consistent with the expectation that the width of the nucleon ground state increases at lighter quark mass.

Now we examine the right plot showing the eigenmodes for the first excited state. Historically it was thought that the first positive-parity excited state coupled strongly to χ_2 . This notion is rejected, as we see that the coupling of χ_2 to the first excited state is negligible at all four smearings. We observe that the dominant contribution is χ_1 at the largest smearing $n = 200$ with a positive sign, with opposite sign contributions from a varying mixture of $n = 35, 100$.

The combination of Gaussians of different width but with opposite sign suggests the possibility of a nodal structure for the first excited state. In order to explore this notion further, we examine the structure of the nucleon and its excitations on the lattice via the Bethe-Salpeter amplitude, referred to hereafter simply as the wave function. As detailed in [14, 15], the baryon wave function is built by giving each quark field in the annihilation operator a spatial dependence,

$$\chi_1(\vec{x}, \vec{y}, \vec{z}, \vec{w}) = \varepsilon^{abc} (u_a^T(\vec{x} + \vec{y}) C \gamma_5 d_b(\vec{x} + \vec{z})) u_c(\vec{x} + \vec{w}), \quad (3.1)$$

while the creation operator remains local. The resulting construction is gauge-dependent, so we choose to fix to Landau gauge. Having established that the contribution of χ_2 is negligible to the ground and first excited state, we obtain the right eigenvectors from a 4×4 correlation matrix analysis using χ_1 only, at the four different smearings. The non-local sink operator cannot be smeared, so we then construct the baryonic wave functions using the right eigenvector u^α only. The position of the u quarks is fixed at the origin and we measure the d quark probability distribution at the lightest quark mass $m_\pi = 156$ MeV.

The left plot of Figure 3 shows the d -quark probability distribution for the nucleon ground state. Recall from the eigenmode analysis that this state is formed from χ_1 , with the two largest

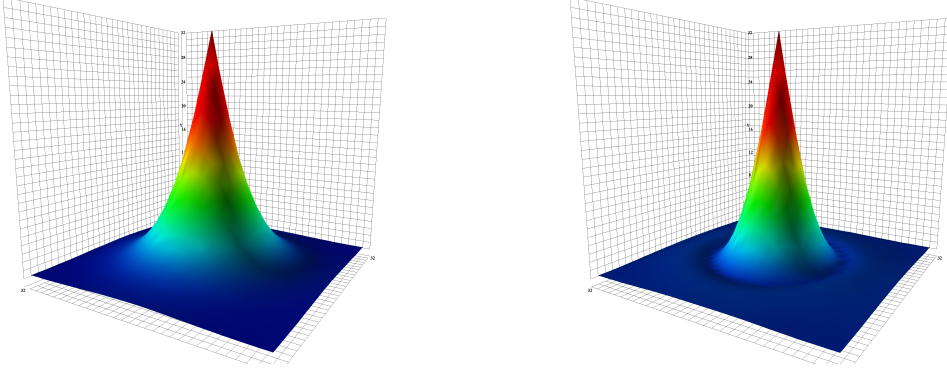


Figure 3: The probability distribution of the d quark about the two u quarks at the origin in the ground state (left) and first excited state (right). The darkened ring around the peak in the first excited state indicates a node in the probability distribution, consistent with a $2S$ state.

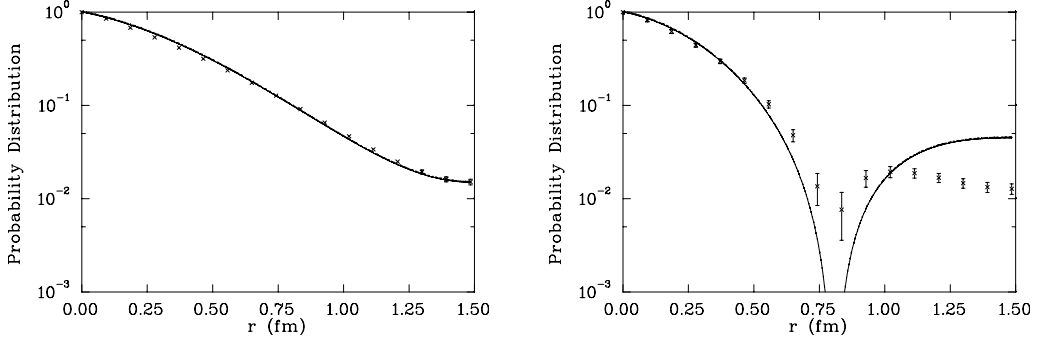


Figure 4: Comparison of the ground state (left) and first excited state (right) d -quark radial probability distribution from our lattice QCD calculation (crosses) with the quark model (solid curve). The quark model predicts the excited state node in approximately the correct location, but deviates at the boundary.

smearings both contributing with a positive sign. In this context, the variational analysis is automatically constructing the nucleon ground state by adjusting the mixture of the $n = 100$ and $n = 200$ operators in order to create a Gaussian of the appropriate width. This interpretation is verified by the simple structure of the ground state wave function.

In contrast, the combination of a wide and narrow Gaussian with opposite sign in the first excited state should yield a nodal structure, and this is indeed what we observe in the right hand plot of Figure 3. The probability distribution of the d -quark in the first excited state clearly shows a single node, as one would expect from a $2S$ radial excitation.

We can gain deeper insight into the first excited state structure by comparing the radial wave function calculated on the lattice with a non-relativistic constituent quark model, based on a one-gluon-exchange motivated Coulomb + ramp potential [16]. The radial Schrodinger equation is solved with boundary conditions relevant to the lattice data, that is, the derivative of the wave function is set to vanish at a distance $L_x/2$.

In order to fix the model parameters, we use a two parameter fit to the ground state lattice radial wave function. This yields a string tension value of $\sqrt{\sigma} = 400$ MeV, with a constituent quark mass of $m_q = 360$ MeV. These parameters are then held fixed for the excited states, and we

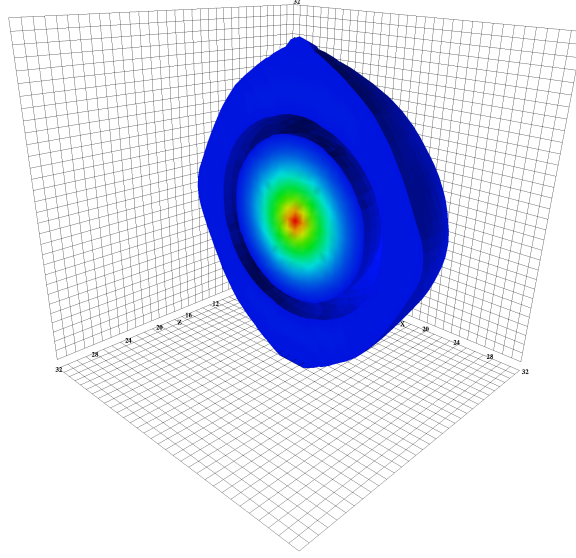


Figure 5: The isovolume of the probability distribution of the d quark in the first excited state. The outer edge can be seen to be affected by the boundary, indicating a necessary finite-volume effect associated with multi-particle components of the state.

can compare the quark model predictions with the lattice data.

In Figure 4, we display the radial wave function predicted by the quark model along with the lattice data. The left plot shows that the quark model is able to fit the lattice ground state relatively well. In the right plot we can now compare the quark model prediction with first excited state radial wave function. We see that the quark model successfully predicts the position of the node, but disagrees with the lattice data as we approach the boundary.

Turning to Figure 5, we examine an isovolume display of the d -quark probability distribution for the Roper. The node structure is clearly visible, and within the node we can see that the distribution has the spherical symmetry that one would expect from a $2S$ radial excitation. However, the outer shell displays significant deviation from spherical symmetry. The finite volume of the lattice and periodic boundary conditions combine to distort what should be a circular shell boundary into a “rounded diamond” shape. This strongly suggests that finite volume effects are responsible for the energy of the lattice Roper state sitting high compared to the experimental value of 1440 MeV. These finite volume effects are also the most likely cause of the significant disagreement with the quark model radial wave function near the lattice boundary.

4. Conclusions

Using a variational analysis consisting of operators constructed with a variety of Gaussian smearings, we find a low-lying positive parity excited state that has a structure consistent with a $2S$ radial excitation of the nucleon, which can therefore be identified as the lattice realisation of the Roper resonance. The radial wave function of the Roper is consistent with the predictions of a constituent quark model. It is clear that at the lightest quark mass there are finite volume effects present in the lattice results, which may cause the state to sit high compared to the mass of

the $N(1440)$ resonance in Nature. Future avenues to explore include a study of the lattice volume dependence of the Roper mass, examining the role that multi-hadron operators can play in constructing a correlation matrix analysis, and probing the electromagnetic structure of octet baryon excitations [17].

References

- [1] N. Isgur and G. Karl, *Hyperfine Interactions in Negative Parity Baryons*, *Phys.Lett.* **B72** (1977) 109.
- [2] N. Isgur and G. Karl, *Positive Parity Excited Baryons in a Quark Model with Hyperfine Interactions*, *Phys.Rev.* **D19** (1979) 2653.
- [3] C. Michael, *Adjoint sources in lattice gauge theory*, *Nucl. Phys. B* **259** (1985), no. 1 58.
- [4] M. Lüscher and U. Wolff, *How to calculate the elastic scattering matrix in two-dimensional quantum field theories by numerical simulation*, *Nucl. Phys. B* **339** (1990), no. 1 222.
- [5] M. Mahbub, A. O. Cais, W. Kamleh, B. Lasscock, D. B. Leinweber, *et al.*, *Isolating Excited States of the Nucleon in Lattice QCD*, *Phys.Rev.* **D80** (2009) 054507, [[0905.3616](#)].
- [6] M. Mahbub, A. O. Cais, W. Kamleh, D. B. Leinweber, and A. G. Williams, *Positive-parity Excited-states of the Nucleon in Quenched Lattice QCD*, *Phys.Rev.* **D82** (2010) 094504, [[1004.5455](#)].
- [7] M. Mahbub, W. Kamleh, D. B. Leinweber, A. O Cais, and A. G. Williams, *Ordering of Spin- $\frac{1}{2}$ Excitations of the Nucleon in Lattice QCD*, *Phys.Lett.* **B693** (2010) 351–357, [[1007.4871](#)].
- [8] M. Mahbub, A. O. Cais, W. Kamleh, B. G. Lasscock, D. B. Leinweber, *et al.*, *Isolating the Roper Resonance in Lattice QCD*, *Phys.Lett.* **B679** (2009) 418–422, [[0906.5433](#)].
- [9] M. S. Mahbub, W. Kamleh, D. B. Leinweber, P. J. Moran, and A. G. Williams, *Roper Resonance in 2+1 Flavor QCD*, *Phys.Lett.* **B707** (2012) 389–393, [[1011.5724](#)].
- [10] B. J. Menadue, W. Kamleh, D. B. Leinweber, and M. S. Mahbub, *Isolating the $\Lambda(1405)$ in Lattice QCD*, *Phys.Rev.Lett.* **108** (2012) 112001, [[1109.6716](#)].
- [11] PACS-CS Collaboration, S. Aoki, K.-I. Ishikawa, N. Ishizuka, T. Izubuchi, D. Kadoh, K. Kanaya, Y. Kuramashi, Y. Namekawa, M. Okawa, Y. Taniguchi, A. Ukawa, N. Ukita, and T. Yoshié, *2 + 1 flavor lattice QCD toward the physical point*, *Phys. Rev. D* **79** (Feb, 2009) 034503, [[0807.1661](#)].
- [12] M. G. Beckett, B. Joo, C. M. Maynard, D. Pleiter, O. Tatebe, *et al.*, *Building the International Lattice Data Grid*, *Comput.Phys.Commun.* **182** (2011) 1208–1214, [[0910.1692](#)].
- [13] S. Güsken, *A study of smearing techniques for hadron correlation functions*, *Nucl. Phys. Proc. Suppl.* **17** (1990) 361.
- [14] D. S. Roberts, W. Kamleh, and D. B. Leinweber, *Wave function of the Roper from lattice QCD*, *Physics Letters B* **725** (2013) 164 – 169, [[1304.0325](#)].
- [15] D. S. Roberts, W. Kamleh, and D. B. Leinweber, *Nucleon Excited State Wave Functions from Lattice QCD*, [[1311.6626](#)].
- [16] R. Bhaduri, L. Cohler, and Y. Nogami, *Quark Quark Interaction and the Nonrelativistic Quark Model*, *Phys.Rev.Lett.* **44** (1980) 1369–1372.
- [17] S. Boinepalli, D. Leinweber, A. Williams, J. Zanotti, and J. Zhang, *Precision electromagnetic structure of octet baryons in the chiral regime*, *Phys.Rev.* **D74** (2006) 093005, [[hep-lat/0604022](#)].